Fachtagung "Experimentelle Strömungsmechanik"
6.–8. September 2022, Ilmenau

Strömungsvisualisierung um einen Seitenspiegel mittels robotischer, volumetrischer LPT.

Flow visualization around an automotive side mirror using robotic volumetric LPT.

Timo Gericke, Steffen Hüttig, Juan Camilo Londono Alfaro
Volkswagen AG, Wolfsburg

Seitenspiegel, Shake-The-Box, Lagrangian Particle Tracking, Roboter, Nachlauf
Side mirror, Shake-The-Box, Lagrangian Particle Tracking, Roboter, Wake

Abstract

Volumetric flow field measurements are obtained to determine the time-averaged properties of the velocity field around a full-scale side mirror in an automotive wind tunnel. Measurements are performed with the MiniShaker Aero consisting of a robot arm and a coaxial volumetric velocimeter (CVV). As tracer particles helium-filled soap bubbles (HFSB) were used. Lagrangian Particle Tracking (LPT) data is analyzed with the Shake-The-Box (STB) algorithm. The aspect ratio of the side mirror is H/W = 0.8. Flow fields were measured at freestream velocities of 33,33 m/s and 22,22 m/s giving a Reynolds number based on the height of the mirror of 357,906 and 238,604. In total the CVV recorded 21 sub-volumes giving a measurement volume of about 430 x 520 x 320 mm (0.072 m³) around the side mirror. Compared to generic side-view mirror models the 1:1 side-view mirror shows different flow structures, especially in the near wake.

Introduction

Reducing drag and acoustic noise are two of the main goals of the automotive industry. A deeper understanding of the dominant flow structures is therefore essential to validate numerical simulations on the one hand and to deepen the understanding of the flow physics on the other hand. Here, robotic volumetric LPT-Measurements are a useful tool to investigate the flow field of such complex bodies like side mirrors compared to planar two-component, stereoscopic and tomographic PIV.
Large-Scale LPT measurements around complex objects require the superposition of a multitude of observation domains (sub-volumes) from different perspectives (Jux et al. 2018). This can only be achieved by a measurement system controlled by means of a robotic arm that does not require calibration after repositioning of the system. Schneiders et al. (2018) introduced a compact coaxial volumetric velocimeter (CVV) also called MiniShaker (LaVision GmbH). The MiniShaker Aero MP is a multi-camera system with four cameras and laser expanding optics ideal for Shake-The-Box, time-resolved volumetric PTV and tomographic PIV.
Shake-The-Box (Schanz et al. 2016) reduces the computational time compared to conventional tomographic PIV by orders of magnitude (factor of 5-8).
Helium–filled soap bubbles enable PIV/PTV measurements in large air volumes. Due to their size of about 300 µm in diameter the scattering intensity of HFSB is about 10,000 times higher

GALA e.V., Karlsruhe, Germany, ISBN 978-3-9816764-8-8

than that of aerosol. Therefore, much larger volumes can be measured or less laser light is necessary. HFSB tracers are neutrally buoyant with a response time of 0.01 ms (Faleiros et al. 2019).
Kim et al. 2020 investigated three different side-view mirrors models using 4D robotic PTV. All three models show a main recirculation zone in the wake. Shape and dimensions are dependent on the shape of the models, as expected. Induced by the low-pressure region in the near-wake, the recirculation zone is a result of the strong downwash flow from the free end. Moreover the recirculation zone is reduced by the inclination angle of the front body. The only model with an undercut effect in the bottom region reduces the vortex region in the mirror wake significantly.
This study describes the robotic volumetric LPT measurements in the wind tunnel facility at Volkswagen. The implementation of the measurement system and the measurement procedure as well as parameters indicating the quality of the measurement like dynamic velocity range (DVR) and dynamic spatial range (DSR) are presented. Finally, the 3D flow field around the side mirror is presented including the main physical properties. To the best knowledge of the authors, this is the first published experimental attempt to measure the 3D flow field around a full-scale side mirror on a full-scale car using the CVV and STB.

Experimental Setup

Measurements are conducted at the closed loop wind tunnel facility of Volkswagen. The atmospheric wind tunnel has an nozzle exit section of 12 m². With a 2 MW electric motor free-stream velocities ranging from 5 to 70 m/s are possible. The test-section is 10 m long and 9.5 m wide. Turbulence intensity of the free stream is ≤ 0.4% and the flow angularity ≤ 0.4 Grad. In the investigated setup the Linear nozzle arrays (LNA), upstream of the car, lead to an increase of the turbulence intensity. Jux et al. (2018) measured a triplication of the turbulence intensity 2 m downstream of a streamlined setup consisting out of four LNAs. Nevertheless, they observed that the seeding rake does not affect the mean velocity by a measureable extend. During the measurements , the wind speed is held constant at 22.22 m/s (Case 1) and 33.33 m/s (Case 2). The car was placed 3 m downstream of the nozzle exit area.

The side-view mirror shown in Fig. 1 has an aspect ratio of 0.7, an inclination angle on the front side of 74 degree and a Reynolds number (Re) defined as Re= $\rho U_\infty H/\mu$ of 357,906 and 238,604. Removable paint (Plasti Dip) was used to paint the whole side mirror and parts of the car black in order to reduce reflections.

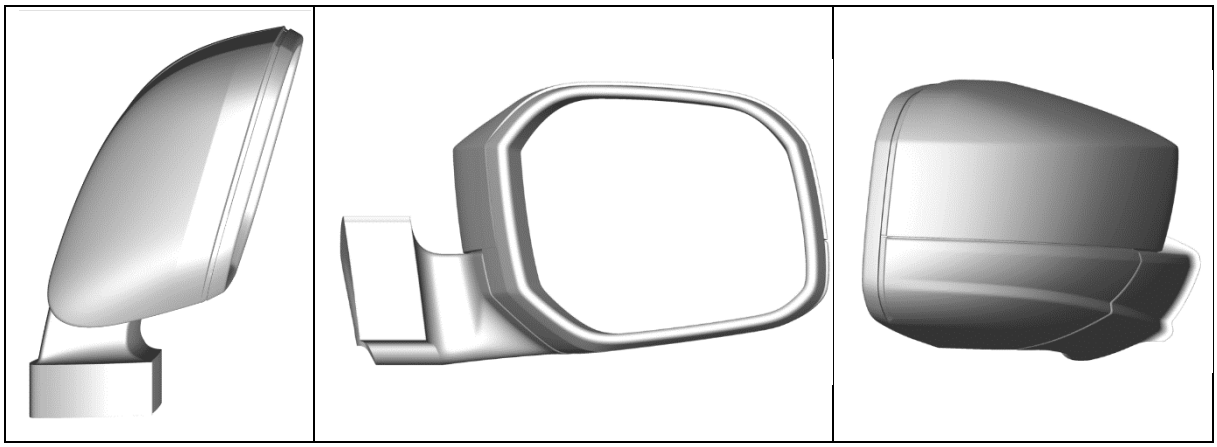

Fig. 1: Side-view mirror in top view (left), rear view (middle) and side view (right).

GALA e.V., Karlsruhe, Germany, ISBN 978-3-9816764-8-8

For the acquisitions of the recordings the CVV probe MiniShaker Aero MP (Fig. 2) from LaVision was used. It exhibits four CMOS-Cameras with a frame rate of 100 Hz at full resolution of 1920 x 1280 pixels with macro planar lenses (f-number = 4, f# = 12 mm) and a pixel pitch Δpx of 4.8 µm. The focal point of the cameras was set at 440 mm from the center of the front cap. In addition, the CVV incorporates a spherical lens for the volumetric beam expansion.

Illumination is provided by a Litron NanoPIV Nd:YAG laser with an output energy of 50 mJ per pulse at a wavelength of 532 nm and a frequency of 100 Hz. Laser light is transmitted with an optical fiber towards the CVV's head. The measurable volume, is bound within the region where the camera views overlap in lateral and vertical direction. At a measurement distance of z = 260 mm, the FOV attains 220 x 130 mm² which extends to 450 x 350 mm² at z = 670 mm. Synchronization between the laser and the cameras is assured by a PTU X from LaVision.
The CVV heads position and orientation is controlled by a robotic arm UR5 from Universal Robots (Jux et al. 2018) with six degrees of freedom (3 rotation and 3 translation axes), similar to the movement range of a human arm. Position repeatability is stated by the manufacturer as ± 0.1 mm (Universal Robots 2014). Maximum reach of the UR5 stretches 850 mm in radius around the robot base.
Helium-filled soap bubbles were used as tracer particles with a mean size of 300 µm. A HFSB generator (Fig. 2) from LaVision was used to generate the seeding particles. The system consists of a fluid supply unit (FSU), one base profile, five linear nozzle arrays (LNAs) and a power supply unit (included in FSU). Span width of the LNA is 874.5 mm with a profile chord of 186.6 mm and a profile thickness of 29.9 mm. In total 20 nozzles are distributed over the span width of the LNA. Each nozzle produces 40.000 soap bubbles per second. In total 4 x 10^6 tracers per second are produced, distributed over a cross section of 200 x 874.5 mm².The seeding rake was placed at the nozzle exit area (Fig. 2).

Fig. 2: Experiment set-up with seeding system (FSU and LNAs) and VCC mounted on the robotic arm.

A single-plane calibration plate (LaVision Type 286-39 SSSP), mounted to optomechanical components, is used for the geometric calibration. The calibration plate consists of 42 dots with a center-to-center spacing of 40 mm and a dot diameter of 12 mm. Geometrical calibration was performed with five different views at z = 440 mm and the pinhole method. After the geometric calibration a volume self-calibration (Wieneke 2008) followed by the determination of the optical-transfer-function (OTF) (Schanz et al. 2012) is performed with the use of experimental data in DaVis 10.2.0.76597.

GALA e.V., Karlsruhe, Germany, ISBN 978-3-9816764-8-8

For particle image recording the robot base is placed 1740 mm away from the car centerline. Measurements are gathered from a total of 21 positions. At each position 1400 images are recorded at a recording rate of 50 Hz.
Raw particle images are pre-processed using the image pre-processing routine in DaVis 10. Main goal of the pre-processing is the removal of background noise from the image in order to have clearly defined particle images with high contrast between the particles and the background. After the image pre-processing the particle images are analyzed with the Shake-The-Box algorithm implemented in DaVis. Approximately 1,500 particles are recorded in every image, corresponding to a particle image density of 0.001 ppp. Every sub-volume contains approximately 1,400,000 tracks (1000 per image pair). After the particles are tracked, the sub-volumes are merged together (Stitching). Afterwards the Lagrangian description of the velocity is converted into a Eularian description through the binning process. The result is the mean velocity vector field. The interrogation window´s size is 64 voxel with 75% overlap resulting in a grid size of 16 voxel (3.4 mm).
The dynamic spatial range DSR is defined as the ratio between the largest and the smallest measurable length scales (Adrian 1997). For the present setup the largest length scale is given by the length of the measured subvolumes and the smallest length scale is given by the smallest used bin size.

$$\overline{DSR} = \frac{326\ mm}{13.7\ mm} = 23.8 \qquad (1)$$

Another important parameter is the dynamic velocity range (DVR). The DVR is defined as the ratio between the maximum resolvable velocity and the minimum one (Adrian 1997). In the present case the ratio between the maximum measured velocity and the measurement uncertainty in the overlapping region of adjacent subvolumes.

$$\overline{DVR} = \frac{37\ m/s}{0.3\ m/s} = 123 \qquad (2)$$

Results

For a deeper understanding of the dominant flow structures, firstly, the results of the 3D mean velocity field around the mirror at two different velocities are shown in Fig. 4. In the near-wake of the side-mirror a recirculation zone is clearly visible. The recirculation zone is a result of the strong downwash flow from the free ends of the mirror, induced by the low-pressure region in this area. Moreover, a deceleration region upstream of the mirror and acceleration regions on the upper and lower half of the side-mirror are present. Differences between Case 1 and Case 2 are very difficult to identify from this rendering. In Fig. 3 the mean velocity field at z/H = 0.59 (top), y/H = 0.79 (center) and x/h = 1.6 (bottom) for both cases are shown for a better comparability. One of the main differences is a slightly upwards movement (in positive z/H-direction) of the near-wake structure for Case 2 together with an inward motion in y/H direction.
Compared to the findings from Kim et al. 2020 the wake behind the 1:1 side-view mirror shows a different flow structure. In Fig. 5 a comparison of the mean streamline fields at z/H = 0.59 (top) and y/H = 0.79 (bottom) is shown. Here, in both cases, two vortices are present in the near-wake. Also, two saddle points are visible, one point occurring in the x-y plane (z/H = 0.59) and one point in the x-z plane (y/H = 0.79). Kim et al. 2020 only observed one vortex in the recirculation zone in the x-y plane for all three models. This might be a direct result of the different geometries.

GALA e.V., Karlsruhe, Germany, ISBN 978-3-9816764-8-8

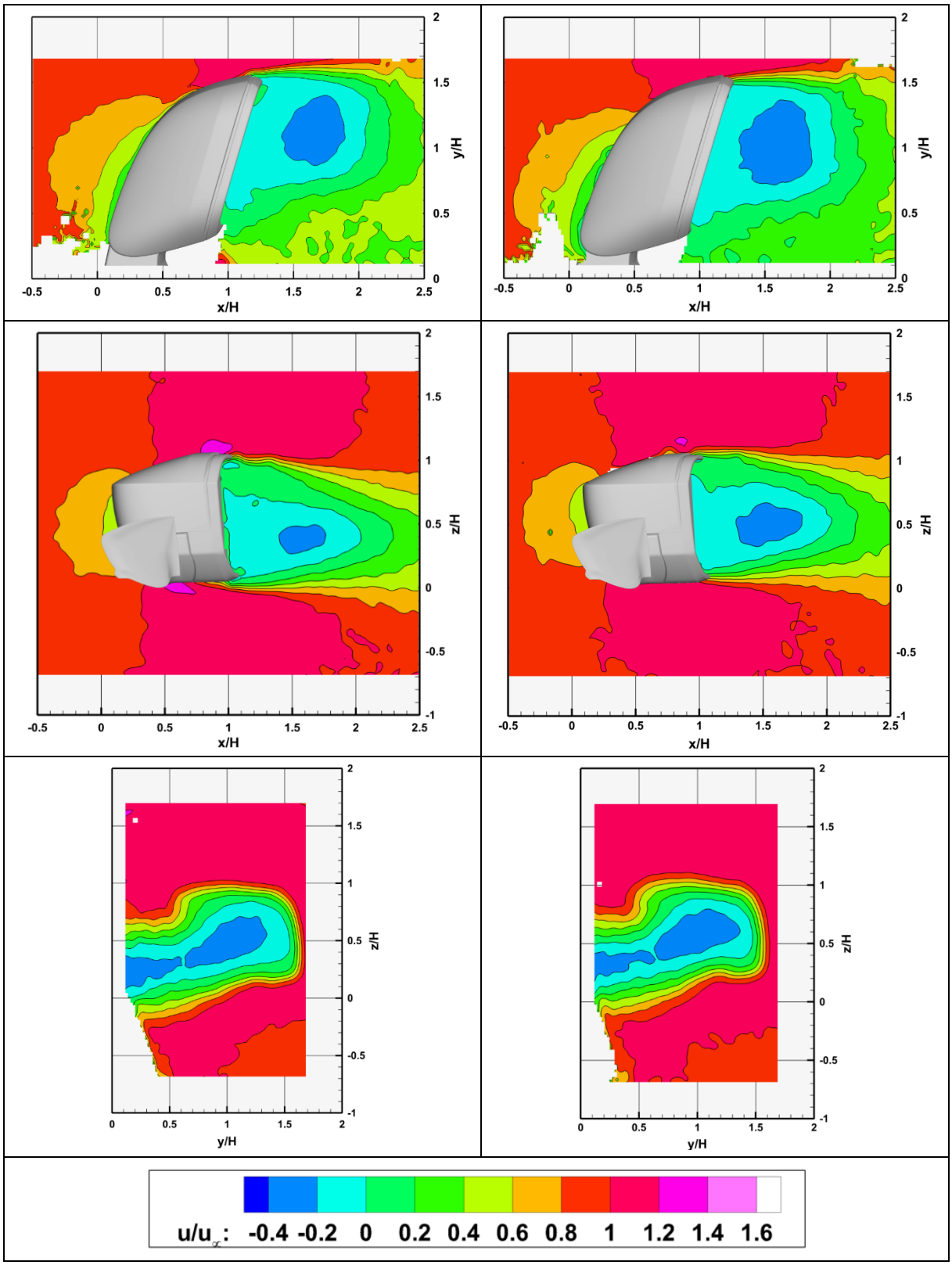

Fig. 3: Mean velocity field at z/H = 0.59 (top), y/H = 0.79 (center) and x/h = 1.6 (bottom) for Case 1 at 22.22 m/s (left) and Case 2 at 33.33 m/s (right) color coded by the streamwise velocity.

GALA e.V., Karlsruhe, Germany, ISBN 978-3-9816764-8-8

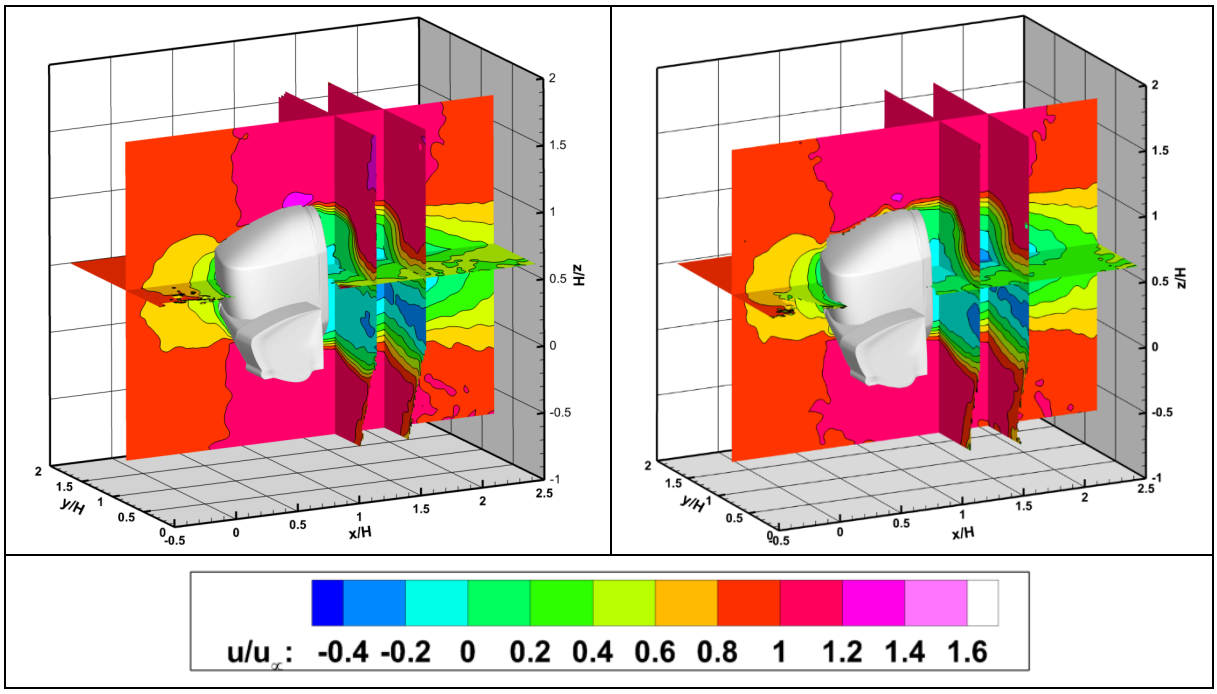

Fig. 4: Result of 3D mean velocity field for Case 1 at 22.22 m/s (left) and Case 2 at 33.33 m/s (right) based on bin-averaging approach and visualized by four perpendicular vector planes color coded by the streamwise velocity.

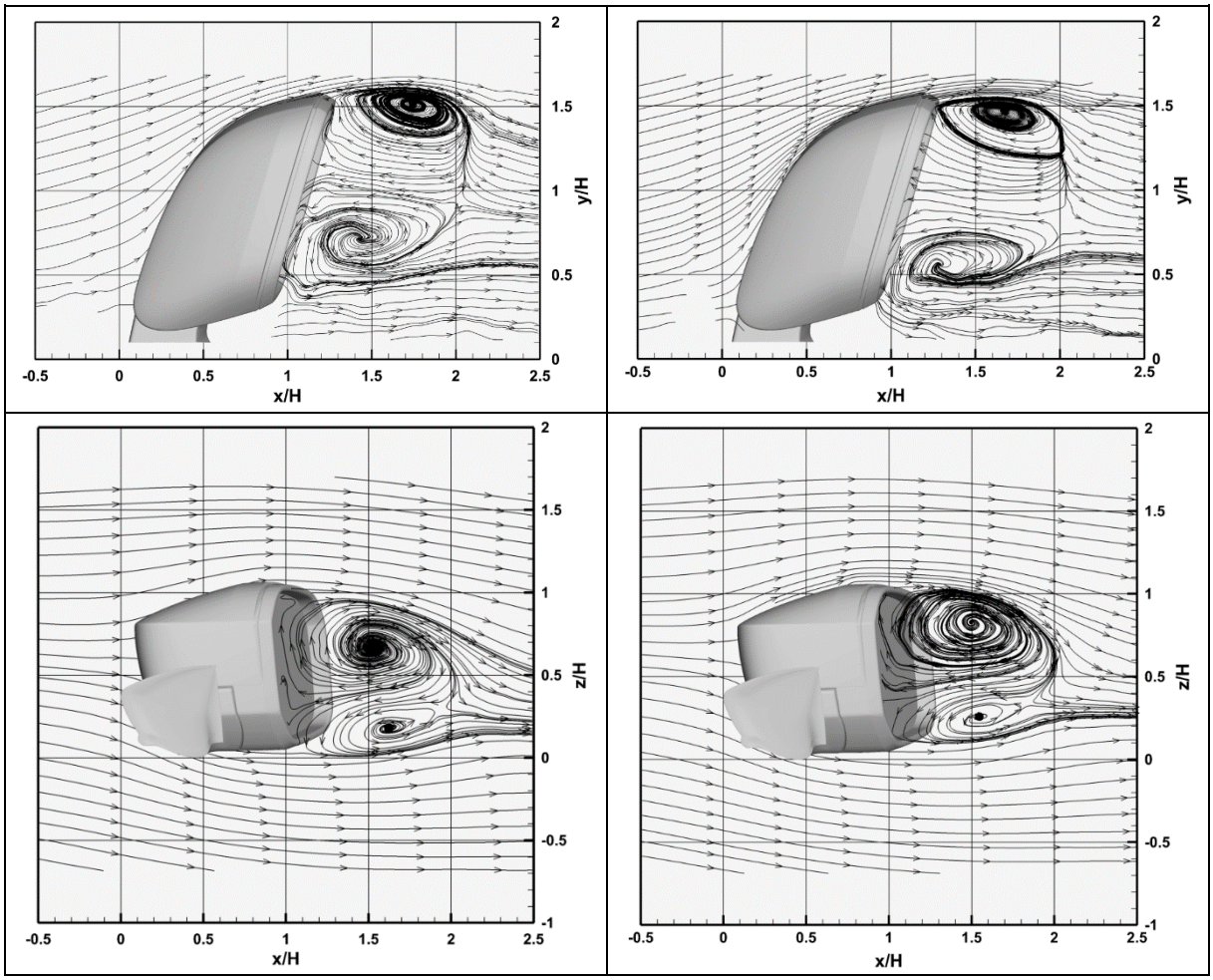

Fig. 5: Mean streamline field at z/H = 0.59 (top) and y/H = 0.79 (bottom) for Case 1 at 22.22 m/s (left) and Case 2 at 33.33 m/s (right).

GALA e.V., Karlsruhe, Germany, ISBN 978-3-9816764-8-8

Conclusion

In the present paper, for the first time, 3D flow measurements of a 1:1 side-view mirror at two different velocities (Case 1 = 22.22 m/s & Case 2 = 33.33 m/s) were performed in order to gain a deeper understanding of the dominant flow structures using robotic volumetric Lagrangian Particle Tracking (LPT). Measurements are performed with the MiniShaker Aero consisting out of a robot arm and a coaxial volumetric velocimeter (CVV). As tracer particles helium-filled soap bubbles were used. LPT data was analyzed with the Shake-The-Box algorithm.
Mean 3D velocity fields and the derived streamline fields were analyzed. It can be seen from the results that for Case 2 the extension of the wake in y/H direction is slightly smaller. This might be a direct effect of the upward motion of the whole recirculation zone of Case 2. A possible reason for the upward motion is the existence or growth of a recirculation bubble on top of the mirror, but this can't be proven with the spatial resolution of the experiment. Here, measurements with a higher spatial resolution are necessary. Compared to the findings from Kim et al. 2020, two instead of one vortices are present in the x-y plane of the near-wake. Here, the different root geometries of the two mirrors lead to the second vortex in Case 2.

The results, opinions and conclusions expressed in this publication are not necessarily those of Volkswagen Aktiengesellschaft.

Acknowledgment

The authors would like to thank the colleagues from Volkswagen Nutzfahrzeuge for their support during the experiments and afterwards.

Literature

Adrian, R. J. 1997: "Dynamic ranges of velocity and spatial resolution of particle Image velocimetry", Meas Sci Technol, 8(12):1393

Faleiros, D.E., tuinstra, M., Sciacchitano, A., Scarano, F., 2019: "Generation and control of helium-filled soap bubbles for PIV", Exp. Fluids 60(3): 40

Jux, C., Sciacchitano, A.; Schneiders, J.F., Scarano, F., 2018: "Robotic volumetric PIV of a full-scale cyclist", Exp. Fluids 59(4): 74

Kim, D., Kim, M., Saredi, E., Scarano, F., Kim, C. K., 2020: "Robotic PTV study of the flow around automotive side-view mirror models", Exp. Therm. And Fluid Sci. 119 (2020)

Schanz, D., Gesemann, S., Schröder, A., Wieneke, B., Novara, M., 2012: "Non-uniform optical transfer functions in particle imaging: calibration and application to tomographic reconstruction", Meas Sci Technol, 24: 024009

Schanz, D., Gesemann, S., Schröder, A., 2016: "Shake-The-Box: Lagrangian particle tracking at high particle image densities", Exp. Fluids 57(5): 70

Schneiders, J.F.G., Jux, C., Sciacchitano; A.; Scarano, F., 2018: "Coaxial volumetric velocimetry", Meas. Sci. Technol. 29: 065201

Wieneke, B., 2008: "Volume self-calibration for 3D particle image velocimetry", Exp. Fluids, 45(4): 549–556

GALA e.V., Karlsruhe, Germany, ISBN 978-3-9816764-8-8